Bonding Changes in Compressed Superhard Graphite[*]

W.L. Mao,[1,4] H.-K. Mao,[1,4] P.J. Eng,[2,3] T.P. Trainor,[2,7] M. Newville,[2]
C.-C. Kao,[5] D.L. Heinz,[1,3] J. Shu,[4] Y. Meng,[6] R.J. Hemley[4]

[1]Department of the Geophysical Sciences,
[2]Consortium for Advanced Radiation Sources (CARS)
[3]James Franck Institute, The University of Chicago, Chicago, IL, U.S.A.
[4]Geophysical Laboratory, Carnegie Institution of Washington, Washington, DC, U.S.A.
[5]National Synchrotron Light Source (NSLS), Brookhaven National Laboratory, Upton, NY, U.S.A.
[6]Advanced Photon Source (APS), Argonne National Laboratory, Argonne, IL, U.S.A.
[7]Department of Chemistry and Biochemistry, University of Alaska, Fairbanks, AK, U.S.A.

Introduction

Because of its ability to form sp, sp^2, and sp^3 hybridized bonds, elemental carbon can exist in a diverse number of forms (e.g., carbynes, graphite, nanotubes, fullerences, and cubic and hexagonal diamond) [1]. The nature of the transition in cold-compressed graphite has been an intriguing and long-standing mystery. There is a dramatic increase in electrical resistivity from metal to insulator [2] above 15 GPa, a sharp drop in optical reflectivity [3, 4], broadening of the higher frequency E_{2g} line involving in-plane displacements above 9 to 15 GPa [4, 5], an increase in optical transmittance above 18 GPa [6], and changes in the x-ray diffraction patterns [7, 8] beginning at 14 GPa. These observations led to speculation on whether this high-pressure phase is hexagonal diamond, an intermediate phase between graphite and diamond, or an amorphous phase [1, 7, 9]. While some aspects of the changes are consistent with hexagonal diamond, unlike the hexagonal diamond form (which can be preserved indefinitely at ambient conditions), the high-pressure form produced in cold-compressed graphite is quenchable only at low temperatures (<100K) [1]. Raman studies of the high-pressure phase do not show characteristic diamond peaks near 1335 cm^{-1} [10], yet studies of the quenched phase exhibit a weak, broad peak in the diamond region [1]. On the other hand, the characteristic graphite Raman peak at 1600 cm^{-1} persists in the high-pressure phase and quenched phase.

Methods and Materials

We ground single-crystal graphite into a fine polycrystalline aggregate, which we loaded into the sample chamber in an x-ray transparent beryllium gasket compressed in a diamond anvil cell (DAC). Pressure was measured by using a ruby fluorescence system [17] at the HP-CAT beamline at the APS. The inelastic x-ray scattering (IXS) experiments were conducted at GeoSoil Enviro Consortium for Advanced Radiation Sources (GSECARS) beamline station 13-ID-C at the APS. X-rays originating from the first harmonic of the APS undulator A were monochromatized by a cryogenically cooled Si (111) double-crystal mono-chromator with an energy bandwidth of approximately 1.1 eV and focused to 80 μm horizontal × 20 μm vertical (full width at half-maximum or FWHM) by a pair of meter-long Kirkpatrick-Baez mirrors. This optics arrangement allows the full undulator beam to fit within the 300-μm-diameter, 50-μm-thick disc-shaped graphite sample loaded between the anvils of the 700-μm-diameter diamond culet. Measurements were performed by scanning the incident beam energy relative to the analyzers with a fixed energy of 9.6865 keV. The inelastically scattered x-ray signals were collected at angles ranging from $2\theta = 18°$-$20°$ with an array of six spherical Si (660) analyzers (50 mm in diameter) on a Roland circle with a diameter of 87 cm, and they were focused to a single detector in backscattering geometry (Bragg angle of 89°). The K edge is probed by the creation of photoelectrons that fill unoccupied electronic states that reduce the energy of the incident photon by an amount equal to the transition energy. Carbon bonds directed along the DAC axis are measured with the analyzer arm in the vertical plane, and those directed perpendicular to the DAC axis are measured with the analyzer arm in the horizontal plane. These two orientations also corresponded to c-axial and a-plane bonding of the polycrystalline graphite, respectively, resulting from the sample developing a very strong preferred orientation under uniaxial compression with graphitic layers aligned perpendicular to the DAC axis (7). Each IXS spectrum took 10 to 12 hours to collect (Fig. 1).

To investigate the structural change while avoiding the complication of strong preferred orientation effects due to uniaxial stress, we conducted an x-ray diffraction study with a helium hydrostatic medium to 24 GPa [19]. Diffraction patterns were taken with monochromatic x-radiation at 37.45 keV and collected with a charge-coupled device (CCD) detector at GSECARS beamline station 13-BM-D and confirmed at HP-CAT beamline station 16-ID-B.
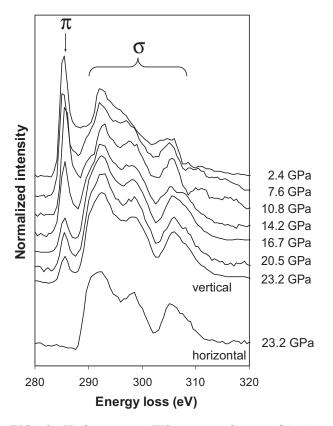
FIG. 1. High-pressure IXS spectra for graphite in horizontal and vertical directions plotted as normalized scattered intensity versus energy loss (incident energy – analyzer energy). The scattered intensity is normalized to the incoming intensity. The lower energy peak, labeled π, corresponds to 1s – π transitions. The higher energy portion, labeled σ, corresponds to 1s – σ* transitions. The bottom spectrum, taken in the horizontal direction, probes bonds in the a-plane and does not show any π-bonding before and after the high-pressure transition. The top seven spectra, taken in the vertical direction, probe the c-plane. After the transition, the σ bonds increase at the expense of the π bonds. © 2003 by Science.*

Results and Discussion

The a-plane spectrum showed only σ-bonding at all pressures and was similar to the control spectrum of the surrounding diamond anvils. The c-axis spectrum showed an additional strong π-bonding characteristic of graphite in electron-energy-loss spectroscopy (EELS) and low-energy x-ray studies [12]. The π-component dropped to half at a pressure of $P >16$ GPa and remained constant to 23 GPa. The observation was inconsistent with a complete conversion to a hexagonal diamond, in which all π-bonds should have converted into σ-bonds. The formation of a hexagonal diamond would require the shift of alternating sp²-bonded honeycomb sheets, which is kinetically inhibited at
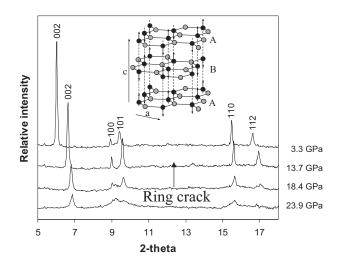

FIG. 2. Hydrostatic x-ray diffraction patterns for graphite compressed at ambient temperature. The diffraction patterns do not show an abrupt transition; instead, there is significant broadening of the diffraction lines consistent with distortion of the basal planes as half of the p-bonds are transformed into s-bonds. The inset of graphite structure shows bridging carbon atoms (black spheres), which are able to pair with an atom in an adjacent layer to form a s-bond. In the process, they move out of plane, as indicated by arrows, causing distortion of the graphite layers. The nonbridging carbon atoms (gray spheres) are not displaced and remain p-bonded to adjacent layers. © 2003 by Science.

ambient temperature [7, 18]. In the alternating honeycomb sheets of graphite, half of the carbon positions have a continuous chain of carbon atoms in all layers throughout the crystal (bridging carbons), and the other half have only carbon atoms in alternating layers (nonbridging carbons). The loss of half of the π-bonds can be explained by the formation of σ-bonds between alternating layers along carbon chains as the layers approach each other upon compression, while the nonbridging carbons (which do not have carbon atoms directly above or below) remain in π-bonding. With negligible shifting of basal planes, the transition requires minimal energy and can be reversed at ambient temperature, as observed.

Above 16 GPa, a discontinuous change occurred, but Bragg peaks persisted and remained traceable to the original graphite pattern (Fig. 2), indicating that the high-pressure form remained in a graphitelike atomic arrangement and was not amorphous. Diffraction peaks broadened; in particular, the in-plane reflections 100 and 110 appeared split and became intense relative to others. The sudden broadening under hydrostatic compression is in full agreement with the partially disordered, buckled layers, and the apparent splitting suggests lower symmetry than hexagonal.

We observed exceptional hardness in the high-pressure phase of graphite, as indicated by the broadening of the ruby fluorescence lines. After releasing pressure from the high-pressure phase (without the He pressure medium), the graphite sample left a ring crack indentation [9] on the diamond anvils following the original boundary of the sample in the gasket (Fig. 3). Ring cracks have only been observed when a diamond anvil is indented by another superhard material, such as an opposing beveled diamond anvil. The occurrence of ring cracks indicates that the high-pressure form of graphite is harder than the strong materials commonly used in DACs (e.g., rhenium gaskets, ruby crystals, and refractory oxides). The reversible, orders-of-magnitude change in strength — from very soft graphite to superhard materials — offers a possibility for intriguing applications as pressure-dependent structural components (for instance, a composite gasket for some high-pressure apparatus) [9].
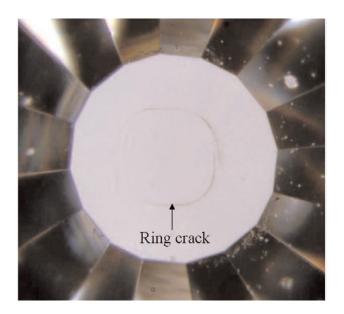

FIG. 3. Photomicrograph showing indention (ring crack) of diamond anvil by the high-pressure form of cold-compressed graphite. © 2003 by Science.

References

[1] E.D. Miller, D.C. Nesting, and J.V. Badding, Chem. Mater. **9**, 18-22 (1997).

[2] E.P. Bundy and J.S. Kasper, J. Chem. Phys. **46**, 3437-3446 (1967).

[3] M. Hanfland and K. Syassen, Phys. Rev. B **40**, 1951-1954 (1989).

[4] A.F. Goncharov, I.N. Makarenko, and S.M. Stishov, Sov. Phys. JETP **69**, 380 (1989).

[5] M. Hanfland, H. Beister, and K. Syassen, Phys. Rev. B **39**, 12,598-12,603 (1989).

[6] W. Utsumi and T. Yagi, Science **252**, 1542-1544 (1991).

[7] T. Yagi, W. Utsumi, M. Yamakata, T. Kikegawa, and O. Shimomura, Phys. Rev. B **46**, 6031-6039 (1992).

[8] Y. Zhao and I.L. Spain, Phys. Rev. B **40**, 993-997 (1989).

[9] F.P. Bundy et al., Carbon **34**, 141-153 (1996).

[10] J. Xu, H.K. Mao, and R.J. Hemley, J. Phys.: Condens. Matter **14**, 11549-11552 (2002).

[11] F.L. Coffman et al., Appl. Phys. Lett. **69**, 568-570 (1996).

[12] G.D. Cody, H. Ade, S. Wirick, G.D. Mitchell, and A. Davis, Org. Geochem. **28**, 441-455 (1998).

[13] H. Shimada et al., Top. Catal. **10**, 265-271 (2000).

[14] M. Cardona and L. Ley, Photoemission in Solids I: General Principles (Springer-Verlag, Berlin, Germany, 1978).

[15] U. Bergmann et al., Chem. Phys. Lett. **369**, 184-191 (2003).

[16] M. Lübbe, P.R. Bressler, D. Drews, W. Braun, and D.R.T. Zahn, Diamond Relat. Mater. **7**, 247-249 (1998).

[17] C.-S. Zha, H.K. Mao, and R.J. Hemley, Proc. Nat. Acad. Sci. U.S.A. **97**, 13494-13499 (2000).

[18] J. Sung, J. Mater. Sci. **35**, 6041-6054 (2000).

[19] K. Takemura, J. Appl. Phys. **89**, 662-668 (2001).

[20] P.F. McMillan, Nature Mater. **1**, 19-25 (2002).

[21] Y. Zhao et al., J. Mater. Res. **17**, 3139-3145 (2002).